Spatial variation of the aftershock activity across the Kachchh Rift Basin and its seismotectonic implications

A P Singh[1,*], O P Mishra[2], Dinesh Kumar[3], Santosh Kumar[1] and R B S Yadav[4]

[1]*Institute of Seismological Research (ISR), Raisan, Gandhinagar 382 009, Gujarat, India.*
[2]*SAARC Disaster Management Centre, New Delhi 110 002, India.*
[3]*Department of Geophysics, Kurukshetra University, Kurukshetra 136 119, Haryana, India.*
[4]*Indian National Centre for Ocean Information Services (INCOIS), Hyderabad, India.*
[*]*Corresponding author. e-mail: apsingh07@gmail.com*

We analyzed 3365 relocated aftershocks with magnitude of completeness (Mc) $\geq$1.7 that occurred in the Kachchh Rift Basin (KRB) between August 2006 and December 2010. The analysis of the new aftershock catalogue has led to improved understanding of the subsurface structure and of the aftershock behaviour. We characterized aftershock behaviour in terms of a-value, b-value, spatial fractal dimension (D_s), and slip ratio (ratio of the slip that occurred on the primary fault and that of the total slip). The estimated b-value is 1.05, which indicates that the earthquake occurred due to active tectonics in the region. The three dimensional b-value mapping shows that a high b-value region is sandwiched around the 2001 Bhuj mainshock hypocenter at depths of 20–25 km between two low b-value zones above and below this depth range. The D_s-value was estimated from the double-logarithmic plot of the correlation integral and distance between hypocenters, and is found to be 2.64 ± 0.01, which indicates random spatial distribution beneath the source zone in a two-dimensional plane associated with fluid-filled fractures. A slip ratio of about 0.23 reveals that more slip occurred on secondary fault systems in and around the 2001 Bhuj earhquake (Mw 7.6) source zone in KRB.

1. Introduction

The Kachchh region is the second most seismically active region in India after the Himalayas. It is considered as pre-continental rifted major sedimentary basin limited by Nagar Parker Uplift (NPU) in the north, Radhanpur–Barmer arch in the east, North Kathiawar Fault (NKF) in the south and eastern Arabian Sea in the west. Its crust consists of Tertiary sediments underlain by Deccan volcanoes, Mesozoic sediments, and Precambrian granitic genesis. The rift basin which is deepening to the south is divided into several sub-basins by numerous faults. Among them the E–W faults which cut across the basins, are deep seated. The intraplate seismicity associated with the ancient rift sedimentary basins has created interest among scientific community to unravel geologic structure, stress distribution pattern and physical processes contributing to the present day seismic activity in the region (Singh *et al* 2011, 2012). The recent studies analyzed key processes involved in the generation of the 1819 Allah Bund earthquake (Gaur 2001), 1956 Anjar earthquake, 2001 Bhuj earthquake and several other earthquakes (Rastogi 2004) (figure 1a, b) of the Kachchh region.

Aftershock sequences are a rich source of information of the earth's crust and source properties of large earthquakes, because of very large number of events occurring over a short period of time in

Keywords. Aftershocks; b-value; fractal dimension; frequency–magnitude; slip ratio.

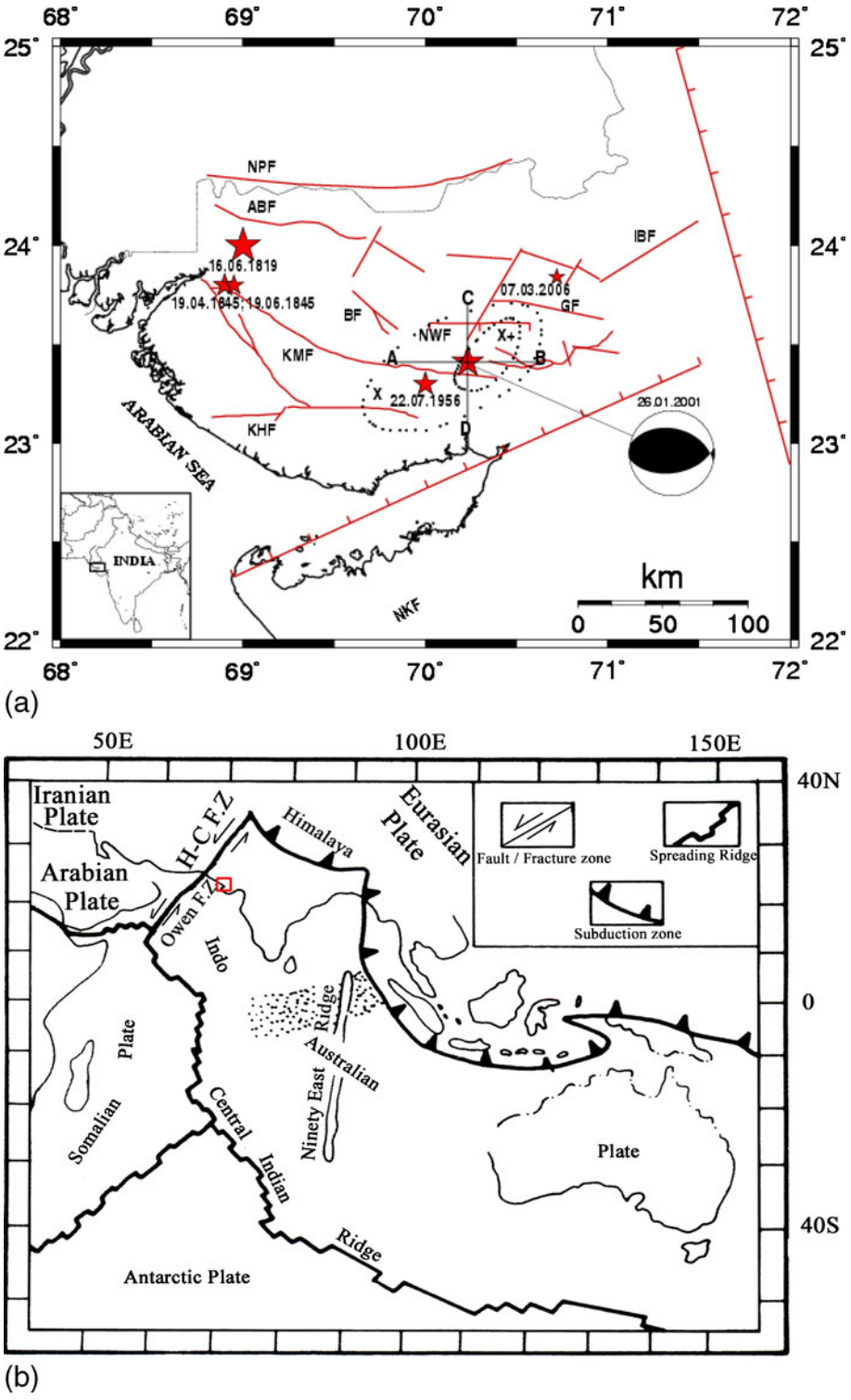

Figure 1. **(a)** A map showing geotectonic setting of the KRB. The 2001 Bhuj main-shock epicenter and past historical damaging earthquakes are shown by red stars. The 2001 fault plane solution is also shown in equal area projection with white (tension) and black (compression) sheds. Faults causing past seismicity in Kachchh region are marked in the figure as: Kachchh Mainland Fault, KMF; Katrol Hill Fault, KHF; Allah Bund Fault, ABF; Old ABF; Island Belt Fault, IBF; Gedi Fault, GF; Banni Fault, BF; North Wagad Fault, NWF; Nagar Parkar Fault, NPF; North Katiwar Fault, NKF. Elliptical areas show distribution of the intensity values X and X^+ during the 2001 Bhuj earthquake. The two solid black lines, AB and CD, indicate locations of the cross sections (after Mishra *et al* 2008). **(b)** Map showing a broader view of regional tectonics of India. The red rectangle represents the 2001 Bhuj earthquake region (after Singh *et al* 2011).

a small area. Several parameters are required to explain crustal heterogeneities and source properties of the mainshock from the aftershocks data which are mainly derived from Gutenberg–Richter relation (1944) or frequency–magnitude empirical equation:

$$\mathrm{Log}\,(N) = a - bM, \tag{1}$$

where 'N' is the cumulative number of events with the magnitude $\geq M$, 'a' is the constant describing the seismic productivity and mechanical coupling or cohesive force between rock masses of the studied area, and b is the slope of the frequency magnitude distribution (FMD) quantifying the ratio of occurrence of small to large earthquakes. In addition to that we have two other statistical parameters namely spatial fractal dimensions (D_s) and slip rate ratio to understand the behaviour of aftershock sequences. Mapping of b-value is an accepted approach to learn about three main natural factors:

- increased material heterogeneity with increase of the b-value,
- increase in shear stress or effective stress with decrease of the b-value, and
- increase in the thermal gradient with increase of the b-value.

Generally, high b-values are observed for highly cracked volumes like magma chamber, reservoir-induced or intraplate sites. However, small b-value is observed for asperities or probable zones for future large earthquakes like plate boundaries (Mogi 1962; Scholz 1968; Warren and Latham 1970; Wyss 1973; Shaw 1995; Jaiswal *et al* 2010). Thus, the b- and a-values shall help in learning about the behaviour of aftershocks, which vary spatially as well as temporally. Fractal dimension (D_s) is a measure of crustal deformation and degree of clustering of earthquakes in space and time (Aki 1981; King 1983; Turcotte 1986; Main 1996). The relation between the fractal dimension (D_s) and b-value is widely discussed (Aki 1981; Wyss *et al* 2004; Mandal and Rastogi 2005). Aki (1981) first showed that these two parameters are related as $D = 3b/c$, where $c \sim 1.5$ is the scaling constant between the logarithm of the moment and magnitude of the earthquake (Kanamori and Anderson 1975). However, a negative correlation between b and D_s is noted in the case of Bhuj earthquake (Mandal and Rastogi 2005). The negative correlation means stress release along faults of larger surface area. Aftershocks occurred two months later than the Bhuj mainshock showed D_s and b-values positive correlation is probably due to numerous smaller shocks releasing stress along faults of smaller surface area.

However, their previous studies on b-value estimates for Gujarat region used limited earthquake datasets. It is worth to mention that their interpretation of these statistical parameters were confined to see only the correlation pattern of b-values with the fractal and slip rate ratio rather than comparing with the seismogenesis of the region. In the present study, a systematic approach has been applied to estimate b-values, a-values, D_s-values and slip rate ratio from relatively large set of homogeneous earthquake data for better correlation of 2-D structural heterogeneity with seismogenesis beneath Kachchh region.

2. Tectonics setting

The Kachchh Rift Basin (KRB) is one among the three major pre-continental rifts including Kachchh, Cambay and Narmada which were formed during the separation of India from the eastern Gondwanaland in the early Cretaceous (figure 1). The sedimentary rift basin is divided into several sub-basins by the east-west trending faults; north dipping Nagar Parkar Fault (NPF) (figure 1) in the north and a south dipping Kathiawar fault in the south are among the major faults bounding the southward deepening sedimentary basin. Besides these, the significant crustal features are Allah Bund Fault (ABF), Island Belt Fault (IBF), Gedi Fault (GF), Kachchh Mainland Fault (KMF) and Katrol Hill Fault (KHF). North-east (NE) and north-west (NW) trending small faults/lineaments and E-W trending uplifts; Kachchh Mainland Uplift, Pachham, Khadir Bela, Wagad and Chobari uplift, surrounded by the depressions like the Banni plain and Rann of Kachchh. These uplifts mostly associated with the higher than average Bouguer gravity anomalies are interpreted as the basement upwraping/volcanic plugs (Chandrasekhar and Mishra 2002). The epicentral 2001 Bhuj earthquake region lies outside the basalt-covered areas of southern Kachchh and its geologic structure consists of Cretaceous, Tertiary and Mesozoic sediments that overlie the Precambrian basement.

3. Seismicity of the Kachchh region

The first Kachchh earthquake of 16 June 1819 (M 8.0), Allah Bund (Dam-of-God) attracted the attention of International Scientific Community (figure 1) (Rajendran and Rajendran 2001) as the co-seismic uplift had evidenced the presence of the Allah Bund fault expression. The crustal blocks to the south and north of the Allah Bund fault are identified as hanging and footwalls,

respectively (Gaur 2001). An excavated scarp identified in shallow trenches across this structure has been interpreted as part of a fold (Rajendran and Rajendran 2001), which resulted in progressive migration of streams towards the formation of a lake at the down dip side of the up-thrust block. On 19 April 1845, the Lakhpat earthquake (M 6.0) with 60 strong aftershocks was followed by earthquake of M 6.3 on 19 June 1845. The Mw 6.1 Anjar earthquake of 21 July 1956, which caused 115 deaths, was the last serious damaging earthquake in this region, prior to Mw 7.6 Bhuj earthquake of 26 January 2001. The focal mechanisms of the Kachchh earthquakes, such as 1956 Anjar earthquake, 1819 Rann of Kachchh earthquake and a few others indicated reverse faulting, suggesting compressional stress field (Chung and Gao 1995). Even after more than 10 years of Bhuj, aftershock activity is still continuing, M 5.7 on March 2006 and M 5.6 on April 2006 events occurred along the neighbouring GEDI (GF, 30 km north of NWF) and NWF fault respectively. These events are largest aftershocks of the 2001 Bhuj sequence (ISR Report 2009). There were more than 37 moderate earthquakes of magnitude ranging from M 4.2 to 6.1 that occurred between 1821 and 2010 in this region (Rajendran and Rajendran 2001; ISR Report 2009). The most recent of these are well located along with others known only by accounts of local damage. It is clear from the above descriptions that Kachchh is still one of the most seismically active areas of northwest India.

4. Seismic data and aftershocks distribution

The catastrophic 2001 Bhuj earthquake has instigated several premier seismological institutes of India and abroad to carry out intense seismological investigations through extensive monitoring of aftershocks in this area by setting their own seismograph network. However, their monitoring was based on isolation using lesser numbers of seismograph stations in their individual seismic network. Our present study deals with relatively comprehensive data recorded by a large number of seismograph stations. The Gujarat Seismic Network (GSNet), operated by Institute of Seismological Research (ISR), had started acquiring data in early 2006 from the network consisting of 50 3-component Broadband Seismographs (BBS) out of which 19 were Very Small Aperture Terminal (VSAT) connected and 46 were Strong Motion Accelerograph (SMA) covering the whole Gujarat state (figure 2). The Broadband stations relay data in real-time to ISR. Six permanent, 10 temporary

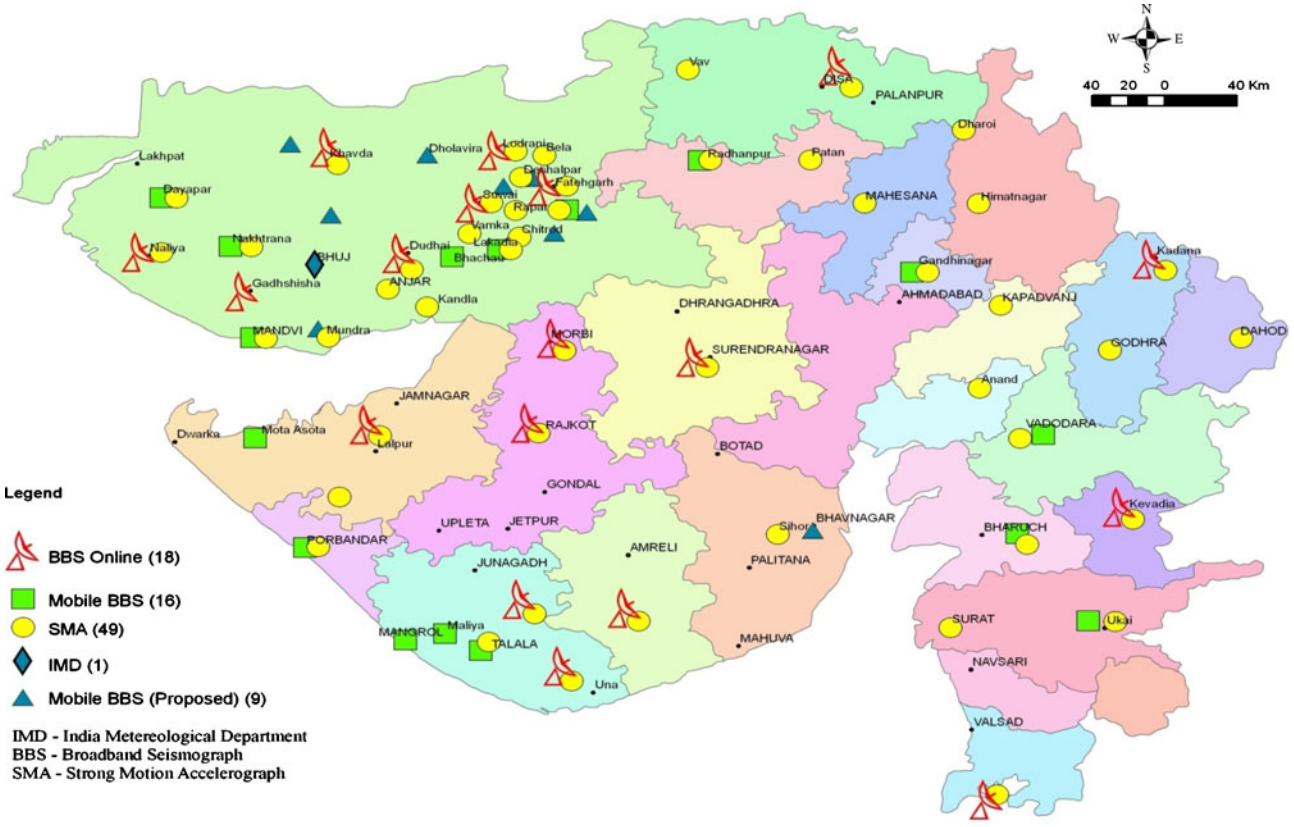

Figure 2. Map shows the distribution of the seismic stations in the state of Gujarat.

BBS and 36 SMA stations are currently installed in the Kachchh district alone, enhancing the network detectability to events with $M \geq 0.8$. The preliminary earthquake information is transferred within 10 minutes after the arrival of seismic waves from the ISR data center to concerned authority of the place. The online data from these stations are available in Guralp format (GCF). However, the data of Reftech and Geon format are received from temporary stations. The online BBS data recorded with 50 samples per second (sps), offline (temporary) BBS data with 100 sps and the SMA data with 100 sps. However, the SMA data fixed is in trigger mode, having a triggering level of 0.002 g. The arrival times of P- and S-phases are picked from the merged datasets consisting of the online and temporary BBS data and all the recorded SMA waveforms. The relocated earthquake estimates are reliable in magnitude and several other parameters that are relevant for earthquake studies. In this study, we analyzed precisely relocated 3365 aftershocks that occurred in the Kachchh region between August 2006 and December 2010 for understanding the subsurface structure and the aftershock behaviour (figure 3).

In order to understand the seismicity pattern of the KRB, initial event locations were obtained

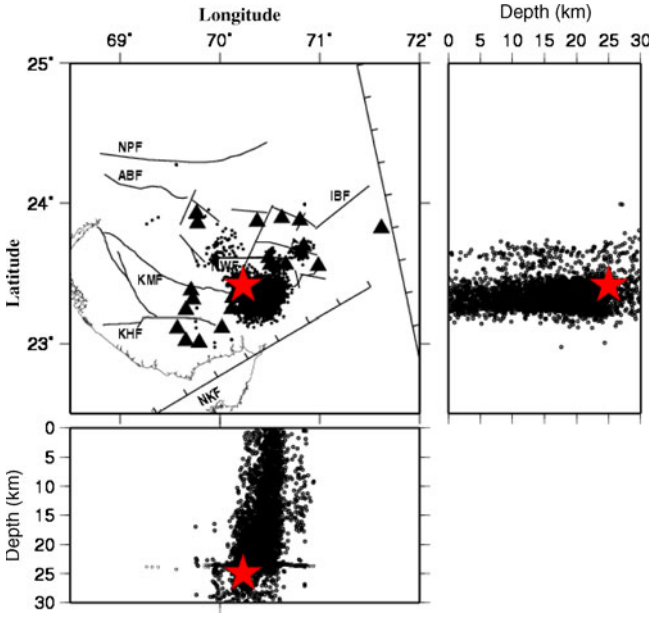

Figure 3. Epicentral distribution of 3365 relocated earthquakes and seismic stations used in this study area is shown by open circles and solid triangles, respectively, in cross-sectional views with depth (the left side shows the distribution of events along latitude with depth, while the lower one shows the distribution along longitude with depth). The figure also shows the identified faults of the regions as denoted in figure 1(a). Depth distribution of the used events (in crosses) in the latitude and longitude directions, respectively. Stars show the 2001 Bhuj epicenter and mainshock hypocenter.

using HYPO71 program (Lee and Lahr 1975). We used a 1-D velocity model of Mandal (2007). The errors in depth decrease to 2.5 km, which may reflect the high quality of data. The root mean square range of the relocated earthquakes is in the range of 0.05–0.2. It is found that the majority of the aftershocks are confined between the KMF and NWF between depths up to 30 km (Mandal *et al* 2004). The overall distribution of earthquakes as a function of depth is shown in figure 3. Our study also revealed that most of the aftershocks occurred at 15–35 km depth, few aftershocks were at less than 10 km (figure 3b, c). The horizontal error in epicenter location by a computer code SEISAN is 1.0–2.0 km while depth error is 2.0–3.0 km. The root mean square error is minimized, stationwise by giving more weightage to clear phases and less weightage to phases which are not clear. Also strong SMA stations phase data are included to have more phase arrivals and good azimuthal coverage.

4.1 *Relocation of aftershock sequences by HypoDD*

We relocated the large set of aftershocks of the 2001 Bhuj earthquake in this study using HypoDD in a similar way as used by Mishra *et al* (2008) in relocating their old dataset (Mishra and Zhao 2003). The double-difference (HypoDD) algorithm incorporates ordinary absolute travel-time measurements and/or cross-correlation of P and S-wave differential travel-time measurements to determine high-resolution hypocentre locations (Waldhauser and Ellsworth 2000). Residuals between the observed and theoretical travel-time differences (or double differences) are minimized for pairs of earthquakes at each station while linking together all observed event-station pairs. A least-squares solution has been used for iterative adjustment of the vector difference between hypocentral pairs. In our study, we used 9975 double-difference data from 3365 earthquakes to relocate the hypocentres by HypoDD. The relocated data show several event clusters (figure 3). We have used a total of five iterations for the conjugate gradient method (LSQR) within the HypoDD inversion technique. In this study, the travel time difference have been estimated for all the event pairs with an inter-event separation less than 8 km and stations located in the range of 100–150 km radius from the clustered centroid. A maximum of 6–8 neighbouring events linked to each other were only considered for the relocation. In effect, HypoDD provides a way of estimating the true errors in locations of shallow events. We analysed the error variations in locations of both shallow and deeper events (table 1), and found that the shallow events (0.0 < depth

Table 1. *Horizontal and vertical errors in relocations of aftershocks using HypoDD.*

Depth of aftershocks	Error in latitude (±km)	Error in longitude (±km)	Error in depth (±km)
0–10	0.00–0.125	0.00–0.226	0.00–2.21
10–15	0.00–0.131	0.00–0.243	0.0–2.833
15–25	0.00–0.312	0.00–0.362	0.0–2.932
25–35	0.00–0.364	0.00–0.335	0.0–3.247
≥35	0.00–0.405	0.00–0.421	0.00–4.081

≤ 15 km) located by HypoDD have lesser horizontal (<0.25 km) and vertical (<3.0 km) errors. However, the error estimates for deeper events (depth >15 km) located by HypoDD are of range (horizontal error ≤ 0.45 km; vertical error ≤ 4.5 km). The relocated aftershocks show a clear geometry of the rupture planes. The rupture dimension is found about 50 × 35 km^2 around the mainshock. The use of relocated aftershocks by HypoDD may not affect statistical analysis of seismicity and 2-D crustal heterogeneities beneath Kachchh region because of a dense spatial distribution of seismic rays on surface as well as in depths (figure 3).

4.2 *Frequency-magnitude distribution or b-value and a-value*

As mentioned in equation (1) a relationship between frequency magnitude distribution (FMD) or mean magnitude is documented by Ishimoto and Iida (1939) and Gutenberg and Richter (1944) on the basis of statistical analysis of a large amount of earthquake data.

It is observed that epicenter maps mostly show that seismicity rate (a-value) is heterogeneous clusters located next to patches without earthquakes. The spatial and temporal variations in b-values are rigorously employed in the investigation of seismotectonics of different seismically active regions of the world. Equation (1) shows that the number of earthquakes declines logarithmetically with the increasing magnitude. The extent rate of this decline is expressed by b-value which is normally close to 1. However, local variations of b-value between 0.6 and 1.5 exist (Ogata and Katsura 1993; Udias 1999). The histogram of magnitudes in the original catalogue compiled by ISR shows a unimodel distribution with some peaks (figure 4). The histogram also reveals the swarm activity up to December 2010. Most of the earthquakes occurred in the magnitude range of 1.5–2.0, which is the first indication of value of magnitude completeness (Mc) of catalogue. We calculated the magnitude of completeness and eliminated all the events having magnitudes less than Mc (figure 5). The calculated Mc was found as 1.7 with 90% goodness-of-fit level. The estimated Mc is based on the assumption of a power-law Gutenberg–Richter relationship and taken as the magnitude where the first derivative of the frequency–magnitude curve has its maximum. Mc can also be defined as the lowest magnitude at

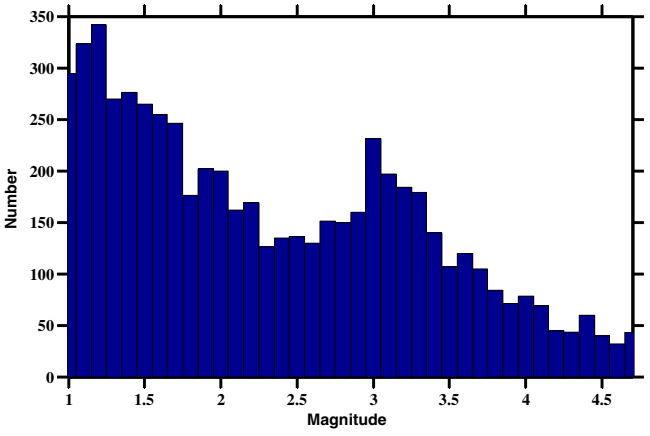

Figure 4. A histogram showing plot of aftershocks of different magnitudes ($M \geq 1.7$) recorded (August 2006–December 2010) and compiled by Institute of Seismological Research (ISR), Gujarat.

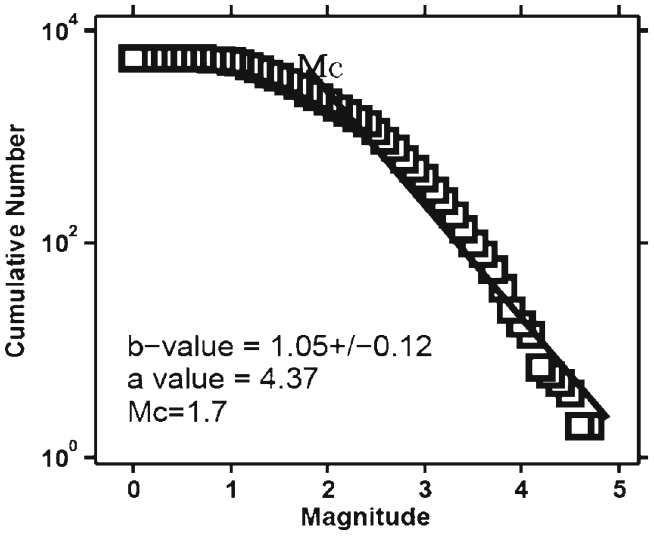

Figure 5. A graph showing frequency–magnitude distribution of G–R relation (log $N = a - bM$) and b-values computed for 0.1 magnitude increment. Mc shows the magnitude of completeness. Solid trianles is non-cumulative number of aftershocks with $M_L \geq 0.1$.

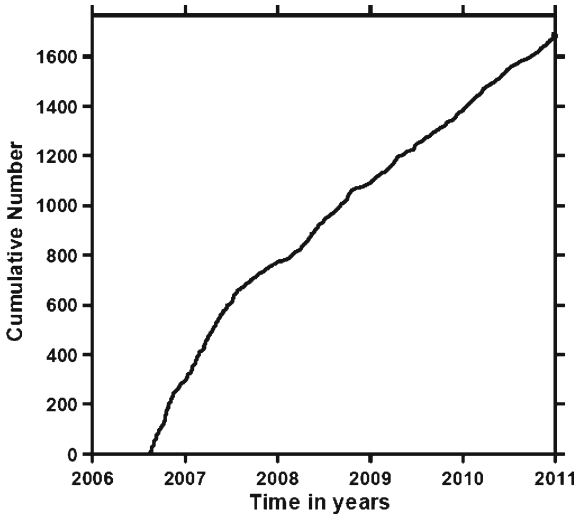

Figure 6. A graph showing the time distribution of the cumulative number of events with magnitude of $M_L \geq 1.7$ as a function of time for the Kachchh region also, corrected for a magnitude shift of dm = 0.3 in 2006.

which 100% of the events are detected in space and time volume (Woessner and Wiemer 2005).

The time distribution of the cumulative number of earthquakes of magnitude 1.7 or more reported in the catalogue for the Kachchh region shows a constant slope with time (figure 6). We interpret this to mean that the reporting was homogenous since August 2006, if the magnitude correction is applied. Software ZMAP following of Wiemer and Wyss (1994, 1997) and Wiemer (1996, 2001) was used to perform the investigation of seismic quiescence. It had permitted interactive event selection in polygons of any shape. ZMAP also allows a custom selection of the size of the grid, latitudinal and longitudinal distance between grid points (grid spacing) in degrees as well as of the number of events per grid point. There is a trade off between the significance of the calculated values and the resolution. Small volumes, meaning few earthquakes, result in better spatial resolution and less reliable values and *vice versa*. The frequency–magnitude plot (figure 5) was used to estimate the parameter *b*-value. Maximum likelihood method is adopted for the calculation of *b*-values following Aki (1965) and Bender (1983). The overall *b*-value estimate for the study area is found to be 1.05 with a standard error of ± 0.12 (figure 5). We also produced maps using the weighted least-squares methods to make sure that results did not depend on the choice of the method to calculate *b*. Our estimation of *b*-value is comparable with the previous values of Mandal and Rastogi (2005) and Yadav *et al* (2005) for this region which suggests a heterogeneous structure of the 2001 Bhuj epicenter region.

Spatial mapping of *b*-value has demonstrated a rich source of information about the seismotectonics of a region. For this purpose, the aftershocks data are projected on to a plane to visualize the frequency–magnitude distribution as a function of space. The *b*-values have been estimated at every node of density spaced grids of $0.50^\circ \times 0.50^\circ$ using 50 to 200 nearest earthquakes considering spatial variation of *Mc* calculated using the approach outlined by Wiemer and Wyss (2002). The size of the grid can also be reduced by limiting the number of earthquakes per sample. However, small sample sizes result in large uncertainties in the estimation of *b*-values. In this study, we found that 50–200 events are sufficient to estimate *b*-values with acceptable error bar. Previous study by Wyss and Weimer (2000) showed that the difference in *b* is larger for samples of 50 events and may be sufficient for statistical significance of the differences. Our *b*-value estimates conspicuously demonstrate that spatial *b*-value varies from 0.6 to 1.4 with standard deviation (δb) in the range of 0.02–0.14 (figure 7a and b), which fall within the tolerable error bar. To a large extent, spatial distribution of *b*-value and standard deviation follow a trend in this study, which is similar as observed by Oncel and Wyss (2000) for Izmit, Turkey earthquake. The low values of spatial standard deviation clearly indicate that the estimated values of spatial *b*-values are statistically significant. The spatial distribution of percentage fit of G–R power law equation has also been calculated by the method given by Wiemer and Wyss (2002) (figure 7c). We estimated *b*- and *a*-values of the G–R law as a function of minimum magnitude, based on the events with magnitude greater than minimum magnitude. We computed a synthetic distribution of magnitudes with the same *b*-, *a*-values and minimum magnitude values, which represent a perfect fit to a power law. Estimate of the goodness-of-fit is made by computing the absolute difference of the number of events in each magnitude bin between the observed and synthetic distribution. Then, we divide it by the total number of observed events to normalize the distribution. The overall spatial variation in percentage fit of GR power law is found to be varying from 60% to 97%, which shows that the estimate of *b*-values, what we made is statistically significant (figure 7c).

Compared to variations in *b*-values for the region, *a*-value shows fewer variations in the region on changing time interval of the data. The *a*-value varies from 2 to 8 and its distribution pattern is similar to that of *b*-value with sharp contrast. The variations in *a*-values do not effectively represent the seismicity status alone. The ratio (a/b) is also estimated for a given magnitude; which indicates periodicity of particular magnitude earthquakes, a useful parameter for the quantification of seismicity for earthquake engineering applications.

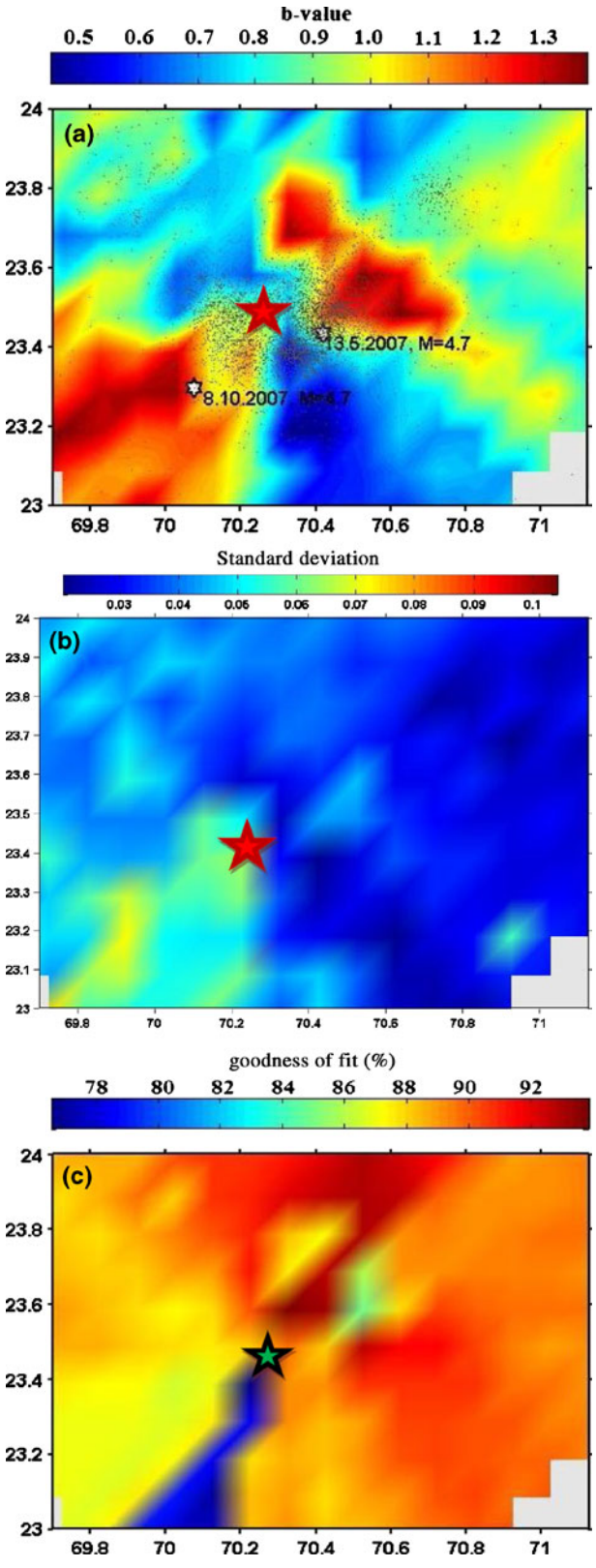

Figure 7. **(a)** Spatial distribution of *b*-value calculated using the maximum likelihood method for the KRB region. Big red star shows 2001 Bhuj mainshock epicenter, two white stars show small earthquakes M 4.7 and solid white circle shows seismicity $M_L \geq 1.7$ pattern in the KRB. **(b)** Standard errors of estimated spatial mapping *b*-value and **(c)** percentage-fit of G–R power law equation. The scales are shown at the top of the each figure.

Estimates of 3D *b*-values mapping in the 2001 Bhuj earthquake region is made by setting up 3-D grids with nodal points separated by 5 km in horizontal and in vertical using fixed number of earthquakes ($n = 150$ for figure 8a and $n = 200$ for figure 8b) ZMAP (figure 8a and b). We calculated *b*-values without limiting the size of the sample volume. To verify that the results are independent of the method used, we mapped *b*-values calculated using both the Maximum Likelihood (ML) and the weighted least-squares (WLS) methods. We note that the spatial patterns observed were the same using the ML and WLS methods. The *b*-value maps shown in figure 8(a and b) are those calculated using the ML method. From 3D *b*-values mapping it is observed that *b*-values in the epicenter region of 2001 Bhuj earthquake vary from 0.45 to 1.21 following the pattern of low-high-low-high-low with depth. Such type of variations in *b*-values with depth suggest that Bhuj earthquake epicenter region consists of highly fractured rock mass of varying structural heterogeneities, which may be a reason for continuous aftershocks activity even after 10 years from the mainshock occurrence. There are two zones of high *b*-values associated with this region at depths 12–16 km and 25–35 km (figure 8a, b). These high *b*-value anomalies are observed in both cases; either *b*-values are calculated using number of earthquake $n = 150$ at every nodes or $n = 200$ suggesting that the existence of anomalies and their positions are well constrained. High *b*-values mapped zones are the zones of a heterogeneous fractured rock mass, possibly associated with low strain energy due to presence of fluids into the rock matrix. The extension of high *b*-value zone from the mainshock hypocenter depth of 25–30 km may suggest the deep crustal source of fluids through the dehydration of the hydroxyl bearing rocks (figure 8a, b). It is spectacular to see that a prominently very high *b*-value above the mainshock hypocenter around the depth of 20 km exists, which may suggest the percolation of meteoric water or sea water into the mainshock hypocenter. This observation is in good agreement with that made by Mishra *et al* (2008). Sandwiched high *b*-value between the top and bottom low *b*-values in the region may have generated sufficient stress to cause the 2001 Bhuj earthquake (Mw 7.6) under the complex geotectonic settings of the region. The existence of this high *b*-value at 20 km depth suggests a homogeneously high stress region that may be a zone of asperity.

The complex pattern of *b*-value changing rapidly within a depth range of 10–35 km indicates tectonic complexity where maximum aftershocks have occurred. Such changes are due to increase in crustal heterogeneities (Aki 1965; Wiemer and Wyss 1997; Wyss *et al* 2004), fluid-filled fractured rock mass.

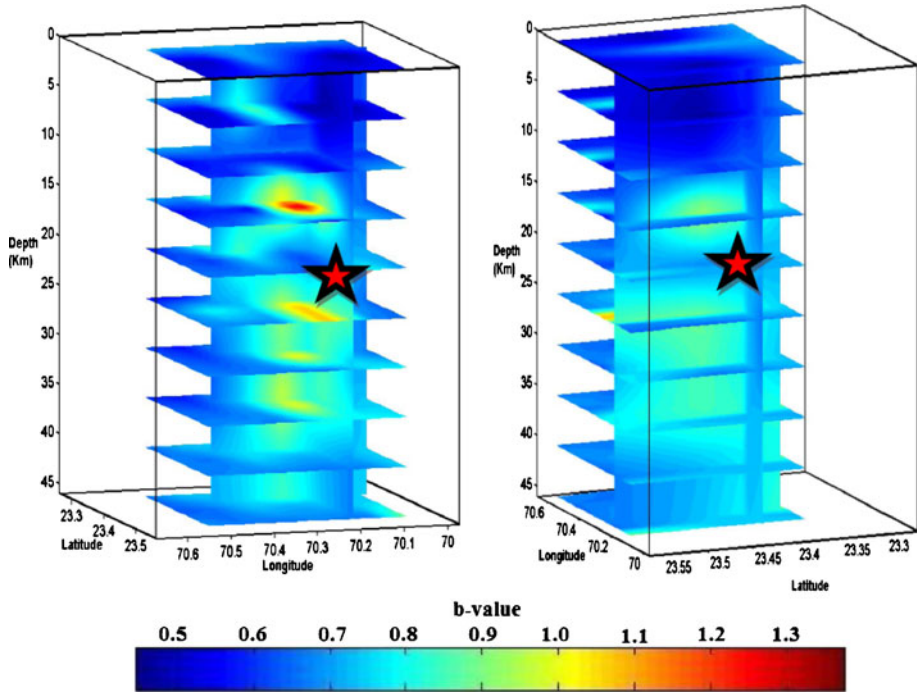

Figure 8. Three-dimensional images of b-values beneath the Kachchh region for selected parts of data of August 2006–December 2010, number of events considered 3447 with $M \geq 1.7$ constant number of events per sample was $N = 150$ and $N = 200$. The scale ranges from 0.5 (dark blue) to 1.4 (bright red). Star shows 2001 Bhuj mainshock hypocenter. The b-values scale is shown to the right of the figure, the range of scale is 0.5–1.4.

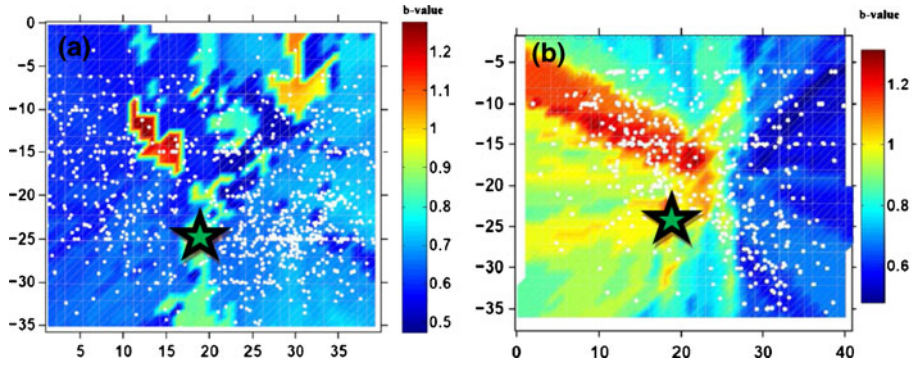

Figure 9. Cross-sectional views, showing distribution of b-values **(a)** along the 2001 Bhuj mainshock (AB), and **(b)** perpendicular to the mainshock (CD). Cross-sectional locations of AB and CD are shown in figure 1(a). The white dots denote aftershocks, while the black star denotes the 2001 Bhuj mainshock hypocentre at depth of 25 km. The red and blue colours indicate high-b and low-b values, respectively. The scale bar is shown to the right of each cross-sectional image as shown under (a) and (b).

The strong heterogeneities within a mafic pluton are responsible for the accumulation of large crustal shear stress that results a lower crustal intraplate earthquake in this region (Kayal *et al* 2002; Mishra and Zhao 2003; Mandal *et al* 2004; Mandal and Pujol 2006; Mandal and Chadha 2008).

The b-values in the north-south (NS) cross sections (positions defined in figure 1) are mapped following gridding technique of Wiemer (1996). It becomes clear that the hypocenters of the mainshocks are associated with high b-values (figure 9a). The east-west cross section also shows that the bottom of the seismogenic crust is associated with anomalously high b-values (figure 9a). The hypocenter plots of the numerous aftershocks in the dataset had obscured the b-value pattern. A very significant pattern of high b-values emerges at the bottom of the east-west (EW) section (figure 9a), despite of its 15 km width. It means that this pattern overrides the differences due to the general heterogeneity visible in figures 7 and 9. It is found that the mainshock of the Bhuj earthquake is strongly stressed up to the surface near the mainshock (figure 7a).

4.3 *Spatial fractal dimension (D_s)*

It is well known that the earthquakes cluster both in space and time, either on a long-term (Kagan and Jackson 1991) or in the short-term time scale (foreshocks and aftershocks). Spatial clustering is examined through the estimation of the spatial fractal dimension (D_s), which describes the spatial distribution of earthquakes and provides a measure of the spatial clustering strength (the smaller the fractal dimension, the stronger the clustering). In order to investigate the spatial properties of the aftershock sequence the fractal analysis based on the correlation integral (Grassberger and Procaccia 1983) is used here.

The correlation integral of a distribution of N earthquakes is:

$$C(R) = \frac{2N_{R<r}}{N\,(N-1)} \tag{2}$$

where $N(R<r)$ is the number of event pairs separated by a distance R smaller than r. If the distribution is fractal, then:

$$C(r) \sim r^{D_s} \tag{3}$$

where D_s is the spatial fractal dimension (or more strictly the correlation dimension, Grassberger 1983). Thus, one can evaluate the fractal dimension of a spatial distribution of earthquakes as the slope of the best-fitted straight line to the log–log plot of $C(r)$ *vs.* r.

The variation in fractal dimension zones gives a lot of information about the geological heterogeneity and stability of the region (Dimitriu *et al* 1993; DeRubeis *et al* 1993). The fractal dimension of spatial distribution of hypocenters is related with the heterogeneity of the fractured material. It characterizes the degree to which the fractals fill up the surrounding space. A value of D_s close to zero may be interpreted as all events clustered into one point, close to 1 indicates the dominance of the sources, close to 2 indicates the planar fractures surface being filled up and a value close to 3 indicates that earthquake fractures are filling up a crustal volume.

In this study, the spatial fractal dimension was estimated from the double-logarithmic plot of the correlation integral and distance between hypocenters, and found equal to 2.64 ± 0.01 (figure 10). The D_s-value higher than 2, although the 3 dimensional space was considered, indicates that the events are randomly distributed into the fault zone crustal volume, whereas much of this volume seems free from hypocenters. Mandal and Rastogi (2005) calculated a spatial correlation of 1.71 ± 0.02 for 2001 Bhuj aftershocks using limited datasets, adjudging this value as indicative for approaching a two-dimensional region. In this study, with D_s = 2.64 and b = 1.05, we found that c = 1.2, which is closer to agreement with the aforementioned statements.

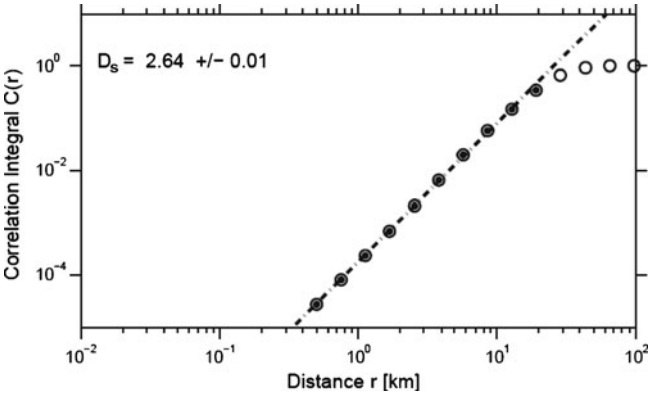

Figure 10. A plot showing correlation integral *versus* distance between hypocenters for Bhuj aftershocks, found equal to 2.64 ± 0.01. The distance ranges for the straight line fits are given as r in frame.

4.4 *Slip ratio estimation*

The amount of slip released during a seismic sequence may be partly attributed to the mainshock and also to the aftershock activity. The slip is relative displacement of formerly adjacent points on opposite sides of a fault, measured on the fault surface forms a major mode of crustal deformation. It has been observed that in general a fraction of the total slip is associated with secondary faults (Khattri 1995). This fraction, called slip ratio, can be estimated from the spatial fractal dimension, D_s according to the formula

$$\frac{S_p}{S} = 1 - 2^{-(3-D)} \tag{4}$$

where S_p is the slip on primary fault and S is the total slip (Khattri 1995; Dimri *et al* 2005). In the case of $D_s = 3$, the total amount of slip is released on the secondary (smaller) faults, whereas in the case of $D_s = 0$, the total slip released on the primary fault. In our case, with $D_s = 2.64$, the slip ratio is found equal to 0.23. This implies that most of the total slip, more than half, was associated with failure on the secondary faults.

5. Results and discussions

The physical cause of aftershock activities is due to the difference of stress level and b-value holds inverse relationship with it (Schorlemmer *et al* 2005). The higher b-values beneath the mainshock could be due to high crack density, high saturation rate, high porosity and strong heterogeneities (Mishra and Zhao 2003; Singh *et al* 2011). In case of low ambient stress, the accumulated stress varies

from very low to the breaking strength levels in contrast to high ambient stress where amplitude of this variation ranges from moderate values to the same maximum breaking strength. The areas of low *b*-values towards NE and NW of the Bhuj mainshock (figures 7, 8a, 8b and 9a, 9b) are most likely characterize high stress accumulation. The state of stress may as well be caused by increased stress in part of the interface due to strong seismic coupling in tectonic regime. The stress gradually accumulates in the rock volume until it slips/ruptures causing a big earthquake and release most of the strain energy. Therefore it is reasonable to suggest that low *b*-value zones are more seismically vulnerable to produce large earthquake. On the other hand, the area with high *b*-value mark low stress accumulation and possibility of earthquake recurrence is more related to *in situ* material heterogeneities rather than stress conditions alone. Around the depth range of 15–35 km the crust is likely to be more extensively cracked (heterogeneous) than elsewhere, where high pore pressure is also probable. Thus high *b*-values could be explained in both ways.

Several researchers explained the possibilities of the fluid near the Bhuj mainshock hypocenter through various geophysical and geological investigations conducted in this region. Recent observations of geomagnetic depth sounding and longer period magnetotelluric investigations inferred as impermeable layer the source area of the Kachchh attaining low resistivity value at a depth range of 0–17 km (Arora *et al* 2002). Recently prepared regional Bouguer and isostatic gravity anomaly maps of the KRB show that the epicenter's deeper source of 2001 Bhuj and the 1956 Anjar earthquakes are associated with the low Bouguer and isostatic gravity anomalies that are distributed between the centers of mass deficiency, causing differential uplifts in this region (Chandrasekhar and Mishra 2002; Mishra *et al* 2005), where our results show high *b*-values (figures 7c, 8 and 9). They explained the gravity lows by the presence of deep-seated mass deficient bodies within the crust or in the upper mantle. The gravity observation and tomography studies of the region support our statistical results that fluid filled fractured rock matrix might have caused the mass deficiency and led to lateral changes in the subsurface density of the host rocks in the 2001 Bhuj hypocentral region (Mishra *et al* 2005). The fractured rock matrix could be an aggregate of mafic intrusive bodies within the crust (Mishra and Zhao 2003; Mandal *et al* 2004; Mishra *et al* 2008; Singh *et al* 2011). The interpretation that the fluids present in the hidden fault zone or percolated to it might have caused high *b*-value at the depth ranges 15–35 km (figure 8a, b). From all the observations in the Bhuj source area, we can infer that fluids were involved in the rupture nucleation and propagation processes of the Bhuj earthquake.

Presence of several active Quaternary fault zone in the Bhuj area and surrounding areas (figure 1) and its nearness to the old (65 Ma) Owen fracture zone from the Arabian Sea as well as to the triple junction between three plates (Arabian, Iranian and Indian plate) may have made the region sufficiently apt to cause permeation of sea/surface water through these active faults and fractures down to deep crust on following fault suction pumping model (Lin *et al* 2003; Mishra and Zhao 2003; Mishra *et al* 2008; Singh *et al* 2011). The cracks within the host rock may have also reinforced by the episodic earthquakes in the Bhuj source region. Mishra (2004) and Mishra *et al* (2008) put forth, for the first time, a similar evidence for fluid driven seismicity by permeation of fluids to the San Andreas source zone due to the existence of nearby Mendicino triple Junction (North America, Pacific and Juan de Fuca plate) has also been reported by Levander *et al* (1998). Fluid pressure and a variety of chemical effects, such as stress corrosion and pressure solution can enhance stress concentration in the seismogenic layer leading to mechanical failure of a strong asperity and thus may have contributed to the nucleation of the Bhuj earthquake.

The spatial distributions of hypocenter of the events associated with this sequence have been studied in terms of fractal dimension. The estimated spatial fractal dimension (D-value) is found equal to 2.64 ± 0.01 that may be interpreted as earthquake fractures are filling up a two-dimensional space of the crust and events are distributed randomly. The estimated fractal dimension and *b*-value follow the well-known Aki (1981) relation of $D=3b/c$, indicating positive correlation between these two parameters.

The slip ratio has been calculated with the help of fractal dimension and it is observed that 23% of the total slip occurred on primary fault whereas major part of the slip occurred on secondary fault systems which reveal that aftershocks occurred on highly fractured rock mass. The geology of the area reveals that high fractures and large heterogeneities are dominant in the epicentral region and fracture density of the area is comparatively higher than that of the surrounding area (Mishra and Zhao 2003).

6. Conclusions

The seismic characteristics of Bhuj sequence have been studied in order to examine seismicity, stress pattern and crustal heterogeneities of the Kachchh region. For this purpose, 3-D distribution of events, *b*-value, *a*-value D_s-value and slip ratio have

been calculated and analyzed using 3850 precisely located events recorded at GSNet of ISR during the period from August 2006 to December 2010. The estimated *Mc* of the catalogue is 1.7 which indicates uniform distribution of earthquakes with time. Most of the aftershocks occurred at 20–25 km depth in high *b*-value zone near the mainshock of the Bhuj earthquake. The 3-D model vindicates the presence of heterogeneities in association with fluids along the fracture zone at this depth range (20–25 km) where the 2001 Bhuj earthquake (Mw 7.6) was nucleated (Singh *et al* 2011, 2012). The pattern of *a*-value is similar to the *b*-value but sharper in contrast. The results are examined with weighted least square of the *b*-value. The spatial distributions of *b*-value distributions suggest increased *b*-values beneath mainshock of the Bhuj earthquake. And also 15–35 km depth in cross section coincides with the maximum occurrence of aftershocks. The high *b*-values at 25 km depth are explained by the presence of fluid fracture zone initiating Bhuj earthquake 2001. The results are not significantly different when we use the weighted least squares fit estimates of *b*-values.

This zone consists of fluid-filled heterogeneous rock mass with high-density fractures that contribute to the observed *Vp*, *Vs* and *Vp*/*Vs* inferred through local earthquake tomography by earlier researchers in the region. The spatial fractal dimension was estimated from the double-logarithmic plot of the correlation integral and distance between hypocenters indicates random spatial distribution and source is a 2-dimensional plan that is being filled up by fractures. We estimate that about 23% of the total slip occurred over the primary fault systems.

Acknowledgements

This study is supported by Ministry of Earth Sciences (MoES), Government of India. The GMT system (Wessel and Smith 1998) is used to plot some figures. APS is thankful to the Director General, ISR for the permission and encouragement to conduct the study.

References

Aki K 1965 Maximum likelihood estimate of *b* in the formula $\log N = a - bM$ and its confidence limits; *Bull. Earthq. Res. Inst.* **43** 237–239.

Aki K 1981 A probabilistic synthesis of precursory phenomena; In: *Earthquake prediction: An international review*; (eds) Simpson D W and Richards P G, AGU, Washington, DC, pp. 566–574.

Arora B R, Rawat G and Singh A K 2002 Mid crustal conductor below the Kutch rift basin and its sesimogeinc relevance to the 2001 Bhuj earthquake; DC-DST News Govt. of India, New Delhi, India, pp. 22–24.

Bender B 1983 Maximum likelihood estimation of *b*-values for magnitude grouped data; *Bull. Seismol. Soc. Am.* **73** 831–851.

Chandrasekhar D V and Mishra D C 2002 Some geodynamic aspects of Kachchh basin and seismicity: An insight from gravity studies; *Curr. Sci.* **83** 492–498.

Chung W Y and Gao H 1995 Source parameters of the Anjar earthquake of July 21, 1956, India, and its seismotectonic implications for the Kutch rift basin; *Tectonophys.* **242** 281–292.

DeRubeis V, Dimitriu P, Papadimitriou E and Tosi P 1993 Recurrent patterns in the spatial behavior of Italian seismicity revealed by the fractal approach; *Geophys. Res. Lett.* **20/18** 1911–1914.

Dimitriu P P, Papadimitriou E E, Papazachos B C and Tsapanos T M 1993 Global study of the distribution of earthquakes in space and in time by the fractal method; In: *Proc. 2nd Cong. Hellenic*; *Geophys. Union, Florina*, May 5–8, 1993, **1** 164–174.

Dimri V P, Vedanti N and Chattopadhyay S 2005 Fractal analysis of aftershock sequence of the Bhuj earthquake: A wavelet-based approach; *Curr. Sci.* **88(10)** 1617–1620.

Gaur V K 2001 The Ran of Kachchh earthquake, 26 January 2001; *Curr Sci.* **80(3)** 17–24.

Grassberger P 1983 Generalized dimensions of strange attractors; *Phys. Lett. A.* **97** 227–230.

Grassberger P and Procaccia I 1983 Characterization of strange attractors; *Phys. Rev. Lett.* **50** 346–349.

Gutenberg B and Richter C F 1944 Frequency of earthquakes in California; *Bull. Seismol. Soc. Am.* **34** 185–188.

Ishimoto M and Iida K 1939 Observations of earthquakes registered with the microseismograph constructed recently; *Bull. Earthq. Res. Inst.* **17** 443–478.

ISR (Institute of Seismological Research, www.isr.gujarat.gov.in) Report (2009).

Jaiswal R K, Singh A P, Rastogi B K and Murty T S 2010 Aftershock sequences of two great Sumatra earthquakes of 2004 and 2005 and simulation of the minor tsunami generated on September 12, 2007 in the Indian Ocean and its effect on Indian Coast; *Nat. Hazards* **57(1)** 7–26.

Kagan Y Y and Jackson D D 1991 Long-term earthquake clustering; *Geophys. J. Int.* **104** 117–133.

Kanamori H and Anderson D L 1975 Theoretical basis of some empirical relations in seismology; *Bull. Seismol. Soc. Am.* **65** 1073–1095.

Kayal J R, Zhao D, Mishra O P, De R and Singh O P 2002 The 2001 Bhuj earthquake: Tomographic evidence for fluids at the hypocenter and its implications for rupture nucleation; *Geophys. Res. Lett.* **29(24)** 2152, doi: 10.1029/2002GL015177.

Khattri K N 1995 Fractal description of seismicity of India and inferences regarding earthquake hazard; *Curr. Sci.* **69** 361–366.

King G 1983 The accommodation of large strains in the upper lithosphere of the earth and other solids by self-similar fault systems: The geometrical origin of b value; *Pure Appl. Geophys.* **121** 761–815.

Lee W and Lahr J 1975 HYPO71 (revised) A computer program for determining hypocenter, magnitude, and first motion pattern of local earthquakes; *US Geol. Surv., Open-File-Report* **75–311** 114.

Levander A, Henstock T J, Meltzer A S, Beaudoin B C, Trehu A M and Klemperer S L 1998 Fluids in the lower crust following Mendocino triple junction migration: Active basaltic intrusion?; *Geology* **26** 171–174.

Lin A, Tanaka N, Uda S and Kumar M S 2003 Repeated coseismic infiltration of meteoric and seawater into deep fault zones: A case study of the Nojima fault zone, Japan; *Geology* **202(1–2)** 139–153.

Main I 1996 Statistical physics, seismogenesis and seismic hazard; *Rev. Geophys.* **34** 433–462.

Mandal P 2007 Sediment thicknesses and Qs *vs.* Qp relations in the Kachchh rift basin, Gujarat, India using Sp converted phases; *Pure Appl. Geophys.* **164** 135–160.

Mandal P and Rastogi B K 2005 Self-organized fractal seismicity and *b* value of aftershocks of the 2001 Bhuj earthquake in Kutch (India); *Pure Appl. Geophys.* **162** 53–72.

Mandal P and Pujol J 2006 Seismic imaging of the aftershock zone of the 2001 *Mw* 7.6 Bhuj earthquake, India; *Geophys. Res. Lett.* **33** 1–4.

Mandal P and Chadha R K 2008 Three-dimensional velocity imaging of the Kachchh seismic zone, Gujarat, India; *Tectonophys.* **452** 1–16.

Mandal P, Rastogi B K, Satyanarayana H V S and Kousalya M 2004 Results from local earthquake velocity tomography: Implications towards the source process involved in generating the 2001 Bhuj earthquake in the lower crust beneath Kachchh (India); *Bull. Seismol. Soc. Am.* **94(2)** 633–649.

Mishra D C, Chandrasekhar D V and Singh B 2005 Tectonics and crustal structures related to Bhuj earthquake of January 26, 2001 based on gravity and magnetic surveys constrained from seismic and seismological studies; *Tectonophys.* **396** 195–205.

Mishra O P 2004 Lithospheric heterogeneities and seismotectonics of NE Japan forearc and Indian regions, D.Sc. thesis, Ehime University, Japan, 223p.

Mishra O P and Zhao D 2003 Crack density, saturation rate and porosity at the 2001 Bhuj, India, earthquake hypocenter: A fluid-driven earthquake?; *Earth Planet. Sci. Lett.* **21** 393–405.

Mishra O P, Zhao D and Wang Z 2008 The genesis of the 2001 Bhuj, India earthquake (*Mw* 7.6): A puzzle for peninsular India?; *Spec. Iss. Ind. Min.* **61(3&4)** 149–170.

Mogi K 1962 Magnitude–frequency relation for elastic shocks accompanying fractures of various materials and some related problems in earthquakes; *Bull. Earthq. Res. Inst.* **40** 831–853.

Ogata Y and Katsura K 1993 Analysis of temporal and spatial heterogeneity of magnitude frequency distribution inferred from earthquake catalogues; *Geophys. J. Int.* **113** 727–738.

Oncel A O and Wyss M 2000 Mapping the major asperities by minima of local recurrence time before the 1999 *M* 7.4 Izmit earthquake; In: *The Izmit and Duzce Earthquakes: Preliminary results*, Istanbul Technical University, Istanbul, pp. 1–14.

Rajendran C P and Rajendran K 2001 Character of deformation and past seismicity associated with the 1819 Kachchh earthquake, northwestern India; *Bull. Seismol. Soc. Am.* **91(3)** 407–426.

Rastogi B K 2004 Damage due to the *Mw* 7.7 Kutch, India earthquake of 2001; *Tectononphys.* **390** 85–103.

Scholz C H 1968 The frequency–magnitude relation of microfracturing in rock and its relation to earthquakes; *Bull. Seismol. Soc. Am.* **58** 399–415.

Schorlemmer D, Wiemer S and Wyss M 2005 Variations in earthquake size distribution across different stress regimes; *Nature* **437** 539–542.

Shaw B E 1995 Frictional weakening and slip complexity in earthquake faults; *J. Geophys. Res.* **100** 18,239–18,252.

Singh A P, Mishra O P, Rastogi B K and Dinesh Kumar 2011 3-D seismic structure of the Kachchh, Gujarat and its implications for the earthquake hazard mitigation; *Nat. Hazards* **57(1)** 83–105.

Singh A P, Mishra O P, Yadav R B S and Kumar D 2012 A new insight into crustal heterogeneity beneath the 2001 Bhuj earthquake region of northwest India and its implications for rupture initiations; *J. Asian Earth Sci.* **48(2)** 31–42.

Turcotte D L 1986 A fractal model for crustal deformation; *Tectonophys.* **132** 261–269.

Udias J 1999 *Principles of Seismology*, Cambridge University Press, Cambridge.

Waldhauser F and Ellsworth W 2000 A double-difference earthquake location algorithm: Method and application to the north Hayward fault, California; *Bull. Seismol. Soc. Am.* **90** 1353–1368.

Warren N W and Latham G V 1970 An experimental study of thermally induced microfracturing and its relation to volcanic seismicity; *J. Geophys. Res.* **75** 4455–4464.

Wessel P and Smith W H F 1998 New version of the generic mapping tools released; *Eos, Transactions, American Geophysical Union* **79** 579.

Wiemer S 1996 Seismicity analysis: New techniques and case studies: Ph.D. Dissertation, University of Alaska, Fairbanks, 150p.

Wiemer S 2001 A software package to analyze seismicity: ZMAP; *Seismol. Res. Lett.* **72** 374–383.

Wiemer S and Wyss M 1994 Seismic quiescence before the 1993 M = 7.5 Landers and M = 6.5 Big Bear (California) earthquakes; *Bull. Seismol. Soc. Am.* **84(3)** 900–916.

Wiemer S and Wyss M 1997 Mapping the frequency–magnitude distribution in asperities: An improved technique to calculate recurrence times?; *J. Geophys. Res.* **102** 15,115–15,128.

Wiemer S and Wyss M 2002 Mapping spatial variability of the frequency–magnitude distribution of earthquakes; *Adv. Geophys.* **45** 259–302.

Woessner J and Wiemer S 2005 Assessing the quality of earthquake catalogs: Estimating the magnitude of completeness and its uncertainty; *Bull. Seismol. Soc. Am.* **95** 684–698.

Wyss M 1973 Towards a physical understanding of the earthquake frequency distribution; *Geophys. J. R. Astron. Soc.* **31** 341–359.

Wyss M and Wiemer S 2000 Change in the probability for earthquakes in Southern California due to the Landers magnitude 7.3 earthquake; *Science* **290** 1334–1338.

Wyss M, Sammis C G, Nadeau R M and Wiemer S 2004 Fractal dimension and *b*–value on creeping and locked patches of the San-Andreas fault near Parkfield, California; *Bull. Seismol. Soc. Am.* **94** 410–421.

Yadav R B S, Shanker D, Singh V P and Gupta S C 2005 On the study of seismic activity of Kutch region and aftershock sequences with reference to Bhuj earthquake, 26th January 2001, India; In: *Symposium on 'Seismic Hazard Analysis and Microzonation'*, Department of Earthquake Engineering, Indian Institute of Technology, Roorkee, India, September 23–24, pp. 119–134.

MS received 26 December 2010; revised 8 September 2011; accepted 22 November 2011